Generalized Central Volume Principle for Recirculation with Contrast Elimination

Jeiran Jahani[1], Glyn Johnson[1], Valerij G Kiselev[2], and Dmitry S Novikov[1]

[1]*Bernard and Irene Schwartz Center for Biomedical Imaging, Department of Radiology, New York University School of Medicine, New York City, New York, United States,* [2]*Department of Radiology, Medical Physics, University Medical Center Freiburg, Freiburg, Germany*

Purpose: To respond to the challenge of tracer recirculation in perfusion measurements, a problem acknowledged since the early days of the method (cf. Ref. 1 and references therein), by creating a framework for analytical modeling of circulation in the whole organism. In particular, the key features of a bolus passage (Fig. 1), which are **(i)** multiple recirculation boluses, and **(ii)** a decaying long-time tail, are related to characteristics of global circulation. We analytically solve three *global circulation models* of increasing complexity (Fig. 2), and select the most adequate one. We also derive exact expressions for the long time tail, generalizing the central volume principle[1] (CVP) to recirculation with contrast elimination.

Target Audience: Quantitative DSC, DCE and CT scientists and clinicians.

Methods: We represent global circulatory system, Fig. 2a, by a few impulse response functions (IRFs) $h_i(t)$ normalized to $\int h_i(t)\,dt = 1$ to enforce contrast mass conservation. The system is stationary and linear. It is convenient to consider the problem in the frequency domain, $h_i(t)\to h_i(\omega)$, such that convolutions become products, the delays t_i are accounted for by the factors $e^{i\omega t_i}$, and the problem maps onto that of linear electric circuits with the currents obeying Kirchhoff laws and governed by the complex-valued admittances $h_i(\omega)$, Fig. 2. This approach naturally incorporates contrast renal elimination/muscular absorption, which we model by the rate $1/\tau$, such that the fraction of contrast remaining after a passage through a lower contour is $\alpha=e^{-t/\tau}$. Thereby, for 1-, 2- and 3-contour (1C, 2C, 3C) models of Fig. 2, we obtain the exact solutions for the Fourier transform $x(\omega)$ of contrast amount $x(t)$ inflowing in the brain (the arterial input function, AIF):

1C: $$x(\omega) = c_0\, e^{i\omega(t_0+t_1)} h_1(\omega) \,/\, [1-\alpha\, e^{i\omega t_1} h_1(\omega)]\,, \qquad (1)$$

2C: $$x(\omega) = c_0\,\lambda\, e^{i\omega(t_0+t_1)} h_1(\omega) \,/\, [1-\lambda e^{i\omega t_1} h_1(\omega) - \alpha(1-\lambda) e^{i\omega t_2} h_2(\omega)]\,. \qquad (2)$$

The geometric series expansions of $1/[1-\ldots]$ yield infinite sums with the terms describing subsequent contrast passages, whose inverse Fourier transforms indeed produce the oscillations in Fig. 1. To derive the overall contrast decay, we note that, since an IRF has a meaning of transit times probability distribution, its frequency expansion near $\omega = 0$ has the following form: $h_i(\omega) = 1 + i\omega\tau_i + [\text{terms higher-order in } \omega]$, where τ_i is the corresponding mean transit time. Plugging this expansion in Eqs. (1) and (2) yields the Lorentzians whose inverse Fourier transforms correspond to $x^{(\infty)}(t)$, the asymptotically exact long-time behavior of $x(t)$ for the two exemplary models, Fig. 2b and 2c [3C model not shown for brevity]:

1C: $$x^{(\infty)}(t)=c_0\, e^{-(t-t_0-t_1)/\tau_e}/(\tau_1+t_1)\,, \qquad \tau_e=\tau(1+\tau_1/t_1)\,; \qquad (3)$$

2C: $$x^{(\infty)}(t)=c_0\lambda e^{-(t-t_0-t_1)/\tau_e}/[\lambda(\tau_1+t_1)+(1-\lambda)(\tau_2+t_2)],\ \ \tau_e/\tau=1+[\lambda(\tau_1+t_1)+(1-\lambda)t_2]/(1-\lambda)\tau_2\,. \qquad (4)$$

We observe that, in contrast to the plateau $x(t)\to\text{const}\neq 0$ representing the classical CVP, the presence of elimination in at least one contour leads to the *overall exponential decay* with the time constant τ_e, which is the essence of the generalized CVP, one of our main results. The classical CVP is obtained by setting the elimination rate $1/\tau=0$. We emphasize that Eqs. (3) and (4) are model-independent: they are valid for *any* $h_i(t)$, and are only determined by the *global topology* of the circulation contours, since we only used the universal low-frequency behavior of the IRFs. To further analyze the DSC MRI data, we use the gamma-variate function for $h_i(t)$, approximate the infinite series in Eqs. (1) and (2) by the first four bolus passes, and substitute $x^{(\infty)}(t)$ from Eqs. (3) and (4) for the rest of them.

MRI: Informed consent was obtained from a glioma patient. GE EPIs of Gd-DTPA administered at a dose of 0.1mmol/kg and rate of 5mL/s were acquired at 1s intervals for first 60s, and at 5s intervals for next 300s totaling 120 samples. Imaging was performed on a 3T Siemens whole body scanner with an 8ch phased array head coil. Parameters: TR=1000ms, TE=32ms, 10 contiguous 3mm thick axial slices, matrix 128×128, FOV=220×220mm^2, FA=30°, BW=1396Hz/pixel, in-plane resolution 1.7×1.7mm^2.

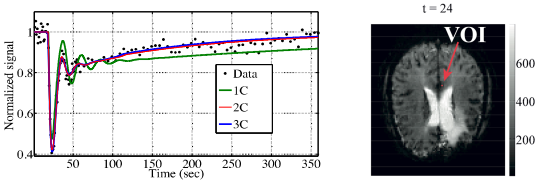

Fig. 1: Signal and model fits (left) of an arterial voxel (right).

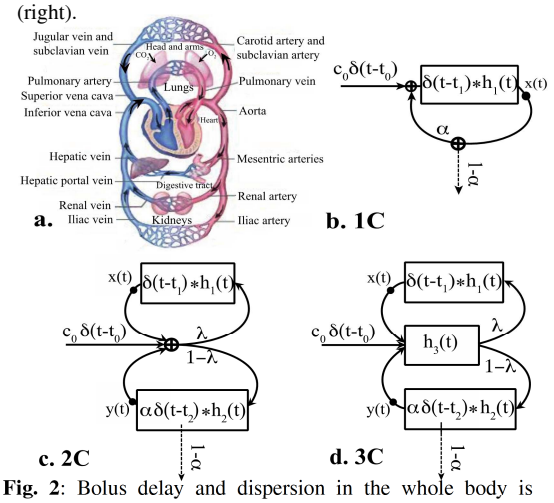

Fig. 2: Bolus delay and dispersion in the whole body is represented by the global 1C, 2C and 3C (compartment) models. The injected contrast flow is a delayed δ-function, with c_0 the net amount of the contrast. The IRFs: h_1 represents brain (our prime focus here), h_2 represents lower body parts (kidney, muscles, legs and their arteries and veins), and h_3 represents heart/lungs. The dashed line indicates contrast renal elimination and muscular absorption. Mass fraction of the contrast entering the carotid artery towards brain is $\lambda\approx 0.2$, while the rest of the body gets $1-\lambda$.

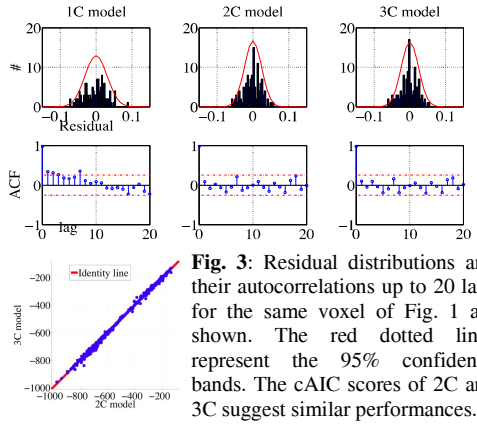

Fig. 3: Residual distributions and their autocorrelations up to 20 lags for the same voxel of Fig. 1 are shown. The red dotted lines represent the 95% confidence bands. The cAIC scores of 2C and 3C suggest similar performances.

Results: All models capture the recirculation boluses as in Fig. 1, but the 1C model cannot explain the fast loss of coherence between oscillations. The heart-pulmonary block h_3 in the 3C model does not improve fit quality much compared to 2C. As shown in Fig. 3, the 2C and 3C residuals comply with our *iid* normal noise assumption, while 1C does not. Residual correlations are mostly random for 2C and 3C, but correlation at 1s lag is about 40% for 1C. Further, 2C and 3C performances are similar according to corrected Akaike Information Criterion (cAIC) scores for over 600 voxels (Fig. 3).

Discussion: From our analysis and overall fit quality, the simplistic 1C model cannot explain the data well. Between 2C and 3C, the less complex 2C was chosen as the candidate model, since the added complexity of 3C does not affect model performance and parameter estimation.

Conclusions: We formulated the first framework in which the contrast recirculation in a given organ (here in the brain) is linked to the topology and quantitative parameters of circulation in the whole organism. In particular, these global features determine the degradation of subsequent boluses and the exponentially decaying tail, thereby generalizing the classical central volume principle onto any recirculation topology and contrast elimination rate. This framework lays the theoretical basis for quantitative perfusion studies using DCE, DSC and CT techniques.

Reference: [1] Zierler K. *Indicator Dilution Methods for Measuring Blood Flow, Volume, etc.* Ann Biomed Eng. 2000: 28(8): 836-848.